Miikki, Kim; Karakoç, Alp; Rafiee, Mahdi; Lee, Duck Weon; Vapaavuori, Jaana; Tersteegen, Jennifer; Lemetti, Laura; Paltakari, Jouni

An open-source camera system for experimental measurements

Published in:
SoftwareX

DOI:
10.1016/j.softx.2021.100688

Published: 01/06/2021

Document Version
Publisher's PDF, also known as Version of record

SoftwareX 14 (2021) 100688

Contents lists available at ScienceDirect

SoftwareX

journal homepage: www.elsevier.com/locate/softx

Original software publication

An open-source camera system for experimental measurements

Kim Miikki [a], Alp Karakoç [b,c,*], Mahdi Rafiee [b], Duck Weon Lee [d], Jaana Vapaavuori [d], Jennifer Tersteegen [b], Laura Lemetti [b], Jouni Paltakari [b]

[a] Aalto University, School of Chemical Engineering, Espoo, Finland
[b] Aalto University, Department of Bioproducts and Biosystems, Espoo, Finland
[c] Aalto University, Department of Communications and Networking, Espoo, Finland
[d] Aalto University, Department of Chemistry and Materials Science, Espoo, Finland

ARTICLE INFO

Article history:
Received 4 December 2020
Received in revised form 10 March 2021
Accepted 15 March 2021

Keywords:
Raspberry Pi
Digital image processing
Non-contact optical measurements
Open-source initiative

ABSTRACT

We present an affordable, yet accurate and modular camera system solution developed on Raspberry Pi 4/4 GB platform with Raspberry v2.x and HQ camera modules with 8 and 12.3 megapixels still resolutions, respectively. The system uses freely available Python scripts and libraries for digital image processing and non-contact optical measurements under MIT licenses as a contribution to the open-source initiative. Several investigations were conducted with the present system, which were two-dimensional (2D) digital image correlation (DIC) for the displacement and strain analysis, the kinetic analysis of the photoisomerization of the spiropyran (a model system for a time-dependent chemical reaction yielding molecules with differing color with respect to starting material) with time-lapse photography, lap shear tests with the assistance of high-speed image capturing and contact (wetting) angle measurements with still images and time-lapse photography. These studies show that the camera system, setups and scripts can be confidently integrated into the chemical, physical and mechanical tests.

Code metadata.

Permanent link	https://github.com/ElsevierSoftwareX/SOFTX-D-20-00089
Legal code license	MIT license
Software code languages and libraries	Python, PiCamera, Matplotlib, Numpy, Scipy, Pandas, Opencv2
Required software for applications which generates scripts	raspistill, raspivid, ffmpeg, mkvmerge
Compilation requirements, operating environments	Image file available for Raspberry Pi 4 single board computers
User documentation, videos, files and manual	mailto:https://github.com/kmiikki/rpi-camera

1. Motivation and significance

Optical tracking and registering systems have been widely used in mechanical, chemical and physical testing such as in strain measurements, ballistic testing, particle velocity tracking and photodegradation analysis [1–5]. Since these systems provide very detailed and accurate visual data that may not be observed by the naked eye due to high speeds or minute variation in wavelengths, they have been increasingly integrated to the conventional measurement protocols, e.g. in automotive, aviation, medical industries and research and academic institutes. However, the prices of optical measurement systems are in general high, which limits their accessibility and use.

For this reason, in this manuscript, we present an open-source multi-purpose camera system initiative, from which researchers all over the world can benefit in their experiments. Considering the cost of commercially available systems and mobility of the hardware, we decided to use the Raspberry Pi 4 /4 GB platform (∼$ 60 as of 09/2020) and camera modules, which are affordable and highly portable. In addition, the mission of Raspberry Pi Foundation, which is providing computational and digital tools, such as intuitive documentations and interactive development environments for Python programming language, was another reason to choose this platform. To elaborate on the details of the conducted research, a general overview of the software and hardware structure is provided with principles and functionalities of

* Corresponding author at: Aalto University, Department of Communications and Networking, Espoo, Finland.
E-mail address: alp.karakoc@alumni.aalto.fi (Alp Karakoç).

https://doi.org/10.1016/j.softx.2021.100688

Table 1
Scripts, libraries and open-source codes used for the illustrative examples.

Operations	Details
Composition	• Recording script: fpsvideo.py • Programs used in the recording script: raspivid (video recording) mkvmerge (conversion from h264 to mkv)
	• Frame extraction script: vid2pic.py • Programs used in the frame extraction script: ffmpeg plugin
	• Region of interest selection script: roi-manual.py
	• Libraries: Imageio, OpenCV-Python
Calibration	• Calibration script: calibratecam.py • Programs used in the calibration script: raspistill (image capturing)
	• Libraries: OpenCV-Python, NumPy, Matplotlib
Exposure	• Exposure script: bracket-exposure.py • Programs used in the exposure script: raspistill (image capturing)
Time-lapse	• Time-lapse script: timelapse.py • Programs used in the time-lapse script: raspistill (image capturing)
Post-processing	Digital Image Correlation (DIC) • DIC analysis program: DICe (open-source code) • Visualization program: Paraview (open-source code)
	Photodegradation • RGB Analysis script: rgbinfo.py • Libraries: OpenCV-Python, NumPy
	Mechanical testing with high-speed image capturing • Angle measurement program: ImageJ (open-source code)
	Contact (wetting) angle analysis • Contact angle measurement script: cadrop.py

the present camera system solution. Thereafter, the experimental measurements, which have been carried out by the authors with different fields of expertise and background, are briefly explained in order to demonstrate the potential of the system. Details of the setup, manufacturing files, scripts and installation guidelines are readily available in the permanent link listed in Table 1. For the flawless installation of the software, the disk image named 'Raspberry Pi camera software suite' is also provided in the repositories, which can be cloned and installed on Raspberry Pi 4 single-board computers.

2. Software description

The present framework and scripts were designed and tested to be used with different versions of Raspberry Pi camera modules. For the ease of access and overview, the code metadata is listed in Table 1. The full script package is provided as an image file in the permanent link provided in Table 1; thus, it is possible to clone and use the image in several Raspberry Pi 4 single-board computers, which drastically minimizes the time and labor for installation. In the following sub-sections, the camera module and some of the work-specific functions are briefly explained.

2.1. Setup and camera modules

The camera system solution was developed to be used modularly for both Raspberry v2.x and HQ camera modules. The Raspberry Pi (RPI) camera module (version 2.x) has an 8 MP sensor with a 1 μs minimum exposure time as depicted in Fig. 1. Two different options for this camera module have been implemented, the first of which is equipped with an IR filter while the second one is without it (namely NoIR). Both modules provide 200 FPS high-speed video recording at VGA resolution and 90 FPS at 720p resolution. On the other hand, the High Quality (HQ) camera module for the RPI released in 2020 has a 12.3 MP sensor, larger sensor area and support for interchangeable lenses. Minimum exposure time for the HQ module is 250 μs (measured with dminexp.py). The CGL 16 mm tele lens with a required C–CS mount provides high quality image and low level of distortion. Minimum focus distance can be shortened to macro photography level with an additional extension tube (C-CS mount). The HQ module provides 120 FPS high-speed video at 1012 $\times$ 760 resolution.

2.2. Software architecture

The camera modules connected to RPI can be used in many ways. This is due to the programmability of the system. There are four applications (raspistill, raspivid, raspiyuv and raspividyuv) which can be used without programming new applications. They have a lot of options and it is possible to make their use much easier with script generation software, which is described in the user manual provided as the Supplementary Material in detail. Another way is to use RPI camera libraries directly and create applications with their functions.

The camera module implementations mainly follow 5 steps: composition, exposure selection, calibration, capturing pictures or videos, and post-processing as schematized in Fig. 2. In the first step, composition and focusing is done with a live preview window. Exposure time should be determined and fixed for consistent pictures. In order to avoid the use of auto white balance, the capturing of images or videos must be calibrated. For this purpose, a white card is used as calibration standard, all combinations of red and blue sensor channel gains within their ranges are captured as images. Their RGB color analysis is done and finally, optimum red and blue gains are calculated when R, G and B channel means are as close as possible to each other as a function of exposure time. The camera suite includes the following post- or preprocessing methods: time-lapse video creation, color analysis, RGB channel splitting and combining, live or still region of interest (ROI) selection, and batch processing.

2.3. Software functionality

2.3.1. Time-lapse and high-speed image capturing

Time-lapse or high-speed videos can be used to observe phenomenon which cannot be studied at normal playback speed. In the first method, the frequency of captured images is lower than the playback frequency; thus, the video is lapsing. The second method, on the contrary, has higher frequency of the captured images than the playback, which results in slow-motion video. Time-lapse images are captured normally as pictures in camera mode with a predefined interval between captures. High-speed pictures are typically captured in video mode, due to its higher data transmission requirement. Several different methods are widely available to create time-lapse or slow-motion videos. In this camera system, time-lapse pictures are captured with timelapse.py, thereafter processed to time-lapse video by gtlvideo.py. High-speed videos are captured and processed with fpsvideo.py. These Python scripts are command-line interface applications for underlying raspistill, raspivid, ffmpeg and mkvmerge.

2.3.2. Digital image correlation (DIC)

The measurement of surface motion and deformation during mechanical experiments is of considerable importance for the mechanical characterization of materials. For this purpose, optical methods using high-speed camera systems have been widely used. Among those methods, digital image correlation (DIC) technique has been a popular method for the analysis

Fig. 1. Camera setups: (a) Raspberry Pi Camera Module v2.x setup, 3-D printed in-house lens mount and Sony IMX219 camera sensor (IR LEDs from left to right: λ_p ~940 nm and λ_p ~880 nm), (b) Raspberry Pi HQ Camera Module setup, original lens mount, Sony IMX477 camera sensor.

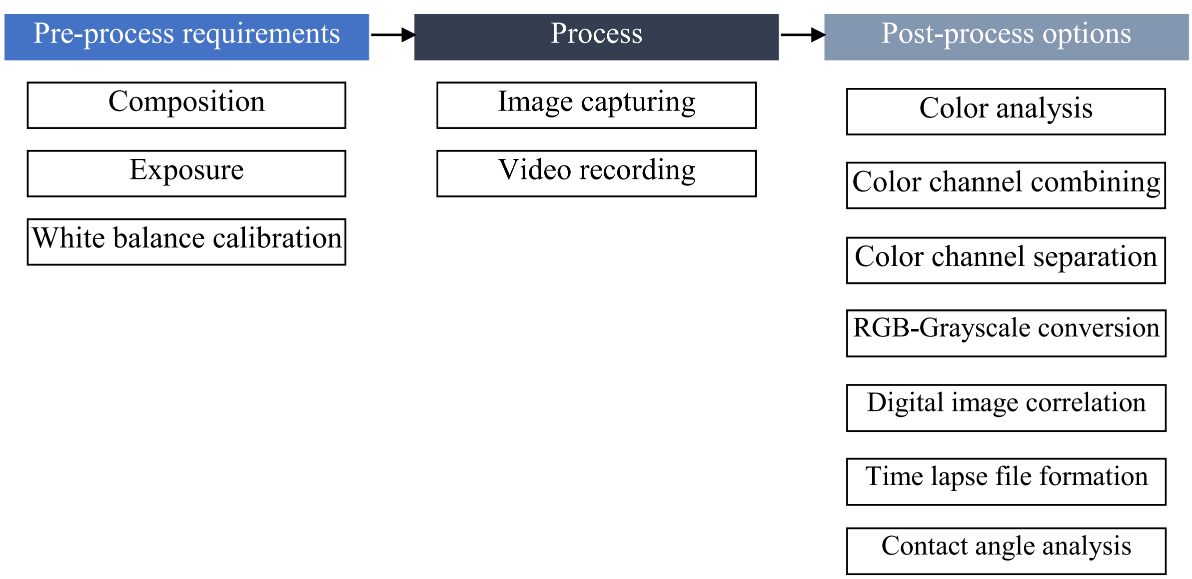

Fig. 2. Camera system workflow comprising required pre-processing functions, main processes of still image capturing, video recording, and post-process functionalities based on the measurement needs.

of displacements and strains during mechanical tests. DIC is a non-interferometric optical method that utilizes the comparison of multiple digital images with respect to the reference image taken during mechanical testing to track the displacement and strain fields of test specimens. Compared to interferometric optical methods that are based on the measurement of the phases of an incident wave and a reflected wave from a surface and the postprocessing of the phase difference, DIC has a much simpler experimental setup. Hence, it has been available commercially and freely in the market, and readily integrated into a variety of applications including tensile tests [6], biomedical applications [7], and measurements of deflection in constructions [8]. Commercial software packages such as VIC from Correlated Solutions StrainMaster from LaVision and GOM Correlate from Zeiss, and open-source DIC codes such as pyDIC by Andre [9], py2DIC by Ravanelli et al. [10], µDIC by Olufsen et al. [11] written in Python, DICE written in C++ by Turner [12], and nCorr written in Matlab by Blaber et al. [13] have been successfully implemented.

The method relies on a speckle pattern on the surface of the specimen which is a random intensity distribution resulting in contrast in the obtained images. Such pattern can naturally exist on or artificially fabricated onto the surface of the specimen. A good speckle pattern should provide high contrast, be random and non-periodic, be isotropic, and have good adhesion to the surface [14]. Multiple methods can be used to fabricate a speckle pattern including spin coating, lithographic methods, and spraying [14]. During specimen testing, patterns are tracked within a timespan as a digital image sequence while the similarity of patterns in each frame is evaluated, e.g., with gradient-based local formulation, fast normalized cross-correlation criterion [12,15].

2.3.3. Contact (wetting) angle measurements

Surface science has been an important field of materials science and engineering in order to understand the surface reactivity and interactions at the surface of matters. For instance, it has been used to analyze the wetting characteristics of paints, inks, adhesives, lubricants, high technology textiles [16–18]. In order to determine the surface energy and characterize the surfaces, i.e. the surface wettability and adhesion, contact angle measurements, referring to the angle formed between solid/liquid or liquid/vapor interface, play an important role in providing quantitative measures. Sessile-drop goniometry for advancing and receding contact angle measurements and tilting plate method for contact angle measurements from the leading and trailing edges of the distorted drop are the commonly used direct measurement methods. In addition to these, for instance, Wilhelmy plate is another method, which indirectly measures the contact angle from the measure force on a thin plate dipped vertically into liquid [19]. The emerging camera technologies and intuitive software libraries such as CAMTIA written in Matlab by Nezerka et al. DropToolKit written in Python by Favier et al. SessileDropAnalysis tool written in Python by van Gorcum, PyDSA written in Python by Launay have great contributions to the current state of the art in open-source contact angle measurement investigations [20–23].

3. Illustrative examples

3.1. Digital image correlation

In order to understand the experimental capabilities and validate the present camera system solution, tensile test experiments were carried out on additively manufactured dog-bone specimens following the dimensional specifications of ISO 527-1:2012 at room temperature (20 °C) and relative humidity of 60%. The force transducer with a limit of 20 kN and speed of 5 mm/min was used with a nominal initial grip to grip separation of 110 mm for the specimens [24]. For the validation of the present system, 2D optical displacement measurements through DIC were performed with Zwick/Roell Z020 tensile testing machine and commercially available StrainMaster DIC system by LaVision. In the commercial system, LaVision Imager pro X camera equipped with Nikon MicroNikkor 105 mm lens was used, for which the dynamic range was 14 bits and the camera sensor size was 1600 × 1200 pixels. The comparative study of strains along Y- axis (e_{YY}) in Fig. 3 indicated that the results obtained from both commercial and the present camera systems matched well.

3.2. Photodegradation

In order to measure the kinetics of the color-changeable material, a coating consisting of 2 wt% of 1′, 3′-Dihydro 1′,3′,3′-trimethyl-6-nitrospiro[2H-1-benzopyran-2,2′-(2H)-indole] (later referred to as 'spiropyran'), purchased from Sigma Aldrich, in poly(vinylpyrrolidone), PVP, purchased from Sigma Aldrich, was spin-coated from chloroform ($CHCl_3$, Sigma Aldrich) solvent on a flexible and stretchable Eco-flex substrate (Ecoflex 00-10, purchased from Smooth-on). The concentration of the spin-coating solution was 2 wt% of PVP in $CHCl_3$ and the applied spin-coating speed was 4000 rpm. When illuminated by UV-light (UV-LED torch, 365 nm, 3 W), the spiropyran underwent a photoisomerization reaction to a merocyanine form, indicated by its color being reversibly transformed from a light purple color to an intense violet (see Fig. 4(a)). When the UV light was turned off, the inverse photoisomerization back to the spiropyran form exhibiting the initial color took place within 20 s of illumination, as shown in Fig. 4(a).

In order to analyze the photoresponse of the spiropyran, its UV–Vis absorbance by using UV–Vis spectrophotometer (UV-2600, Shimadzu co. Japan) was measured before and after UV light exposure (Fig. 4(a) and (b)). The largest absorbance peak was observed near 541 nm, which was assigned to the zwitterionic merocyanine form of the chromophore [26]. To follow the kinetics of the color change, RGB analysis for the photographs taken by a time-lapse code was conducted. The average red (R), green (G), and blue (B) values for the photoisomerization of the merocyanine back to spiropyran as a function of time (s) are shown in Fig. 4(c). As a function of time, the average G value was steeply increased until saturating at approximately 20 s, accompanied by a minor increase in the B channel values. This was in accordance with the green channel being the best indicator for a decrease of the merocyanine absorbance band at 541 nm.

The spiropyran-merocyanine photoisomerization reaction here was taken as a model system for any chemical reaction yielding a substance having a different absorption spectrum as compared to starting materials. Taken into account the maximum time resolution obtained by the present high speed camera systems, the same time range as covered by the state-of-the-art laboratory UV–Vis spectrometers can be measured. Thus, combining high-speed camera imaging and RGB analysis can serve as an easy characterization method for the kinetics of these reactions, including application, such as photodegradation (bleaching) or thermal degradation of materials when exposed to outdoor conditions. The clear advantage over UV–Vis spectrometry is the portability of the camera system, which makes it possible to measure the reaction kinetics of the materials directly where the reaction takes place, such as measuring the photodegradation of a dye-sensitized solar cell placed on the roof of a building.

3.3. Mechanical testing with high-speed image capturing

Testing a lap shear sample for its mechanical properties contains much more information than just the adhesive strength the machine gives. Since testing usually takes only a few seconds, it is hard to get any visual information of for example bending or the fracture mode just by observing it. Lap shear tests can be heavily affected by bending that occurs during the measurement. If bending occurs, not only shear stress but also peel stress affects the sample. This results in a specific distribution of the stress on the samples [27].

In order to better analyze the mechanical testing, the measurement can be recorded with a high-speed camera. The previously described open-source camera system offers optimal possibilities for that. Since it is highly movable it can be mounted in different ways on the mechanical tester to capture videos from various perspectives. Obtained videos can then be analyzed to quantify for example the fracture mode of the lap shear sample.

Lap shear samples were prepared by gluing cellulose plates together. Those were then cut into 1 cm wide and 10 cm long samples prior to measuring. The glue area, located in the middle of the sample, covers 1 cm^2. Samples were measured with

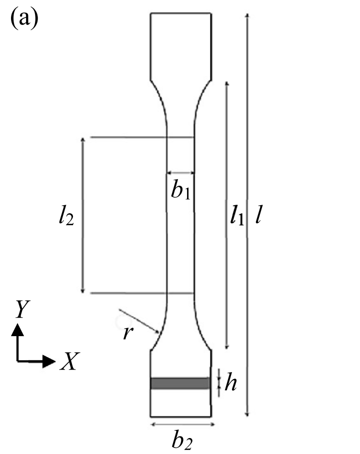

Details	Dimension (mm)
Full length, l	170
Grip face length, l_1	112
Parallel test length, l_2	80
Grip section width, b_2	20
Parallel section width, b_1	10
Thickness, h	4
Radius, r	20

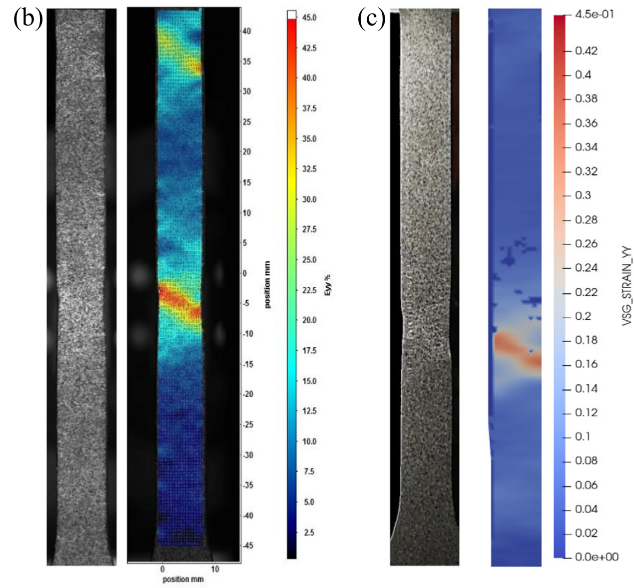

Fig. 3. Digital image correlation comparison for strain (e_{YY}) under uni-axial tension along Y-axis: (a) dimensional specifications of the specimen according to ISO 527-1:2012 [24], (b) image captured with LaVision Imager Pro X camera and analyzed with StrainMaster DIC system, (c) image captured with the present camera module, analyzed with the open-source digital image correlation tool DICe [12] and visualized with ParaView [25].

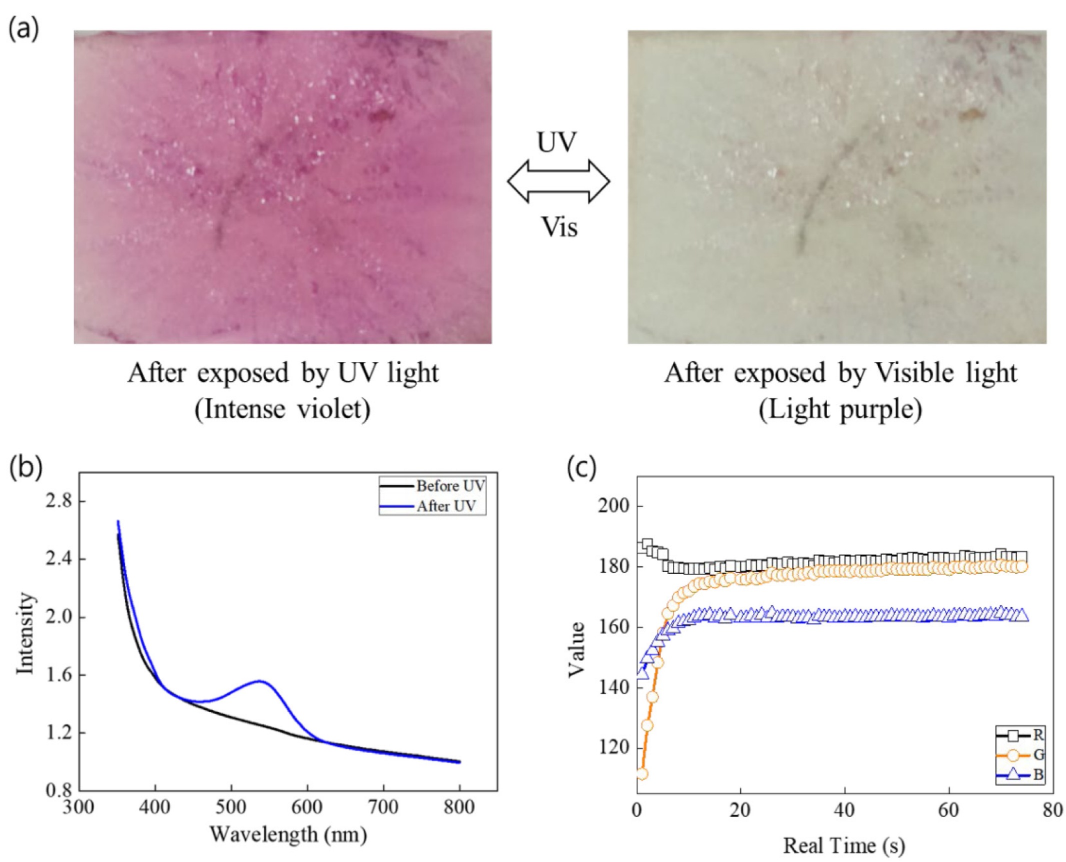

Fig. 4. (a) Optical images of reversible color change, (b) change in absorbance, (c) RGB analysis of the 1′ 3′ -Dihydro-1′ 3′ 3′ trimethyl-6-nitrospiro on the Eco-flex after exposed by UV and visible light. (For interpretation of the references to color in this figure legend, the reader is referred to the web version of this article.)

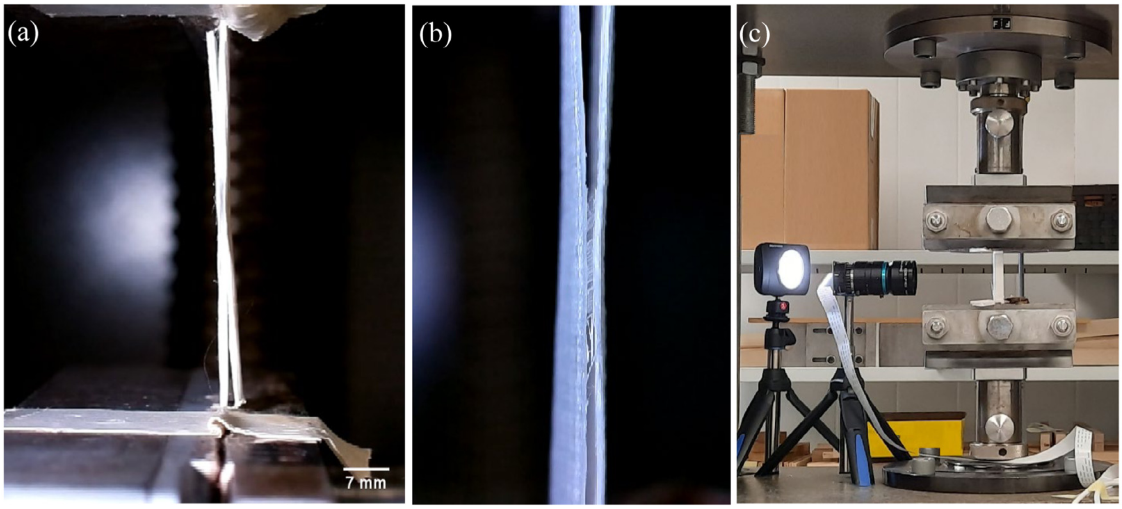

Fig. 5. Mechanical testing with high-speed image capturing: (a) analysis of bending of lap shear sample during mechanical testing, (b) analysis of tear-out at the breaking point, with 1-cm-wide glue area. The videos were recorded with the RPI camera module equipped with a tele-lens and in case of the fracture area additionally with three close-up lenses (+4, +2, +1 dpt), (c) the camera setup.

10 mm/min speed. The video recording was carried out on two different occasions with two different camera setups. For both setups, the camera system was operated by fpsvideo.py python script. The first one was used to analyze the bending of the samples. For this, the whole sample needs to be visible (Fig. 5(a)). The camera perspective shows the sampleś cross-section. Recording was done with the camera module connected to RPI and a tele-lens. The camera was placed on the mechanical tester with a tripod. Optimal lighting was ensured by a 550 lux flicker free LED light on a tripod. Video was recorded with imx477 sensor, 1012 × 760 resolution, 120 frames per second, 2.5 ms shutter speed and AWB (auto white balance) auto-mode. In order to analyze the bending of the sample, the last image before it breaks was extracted from the video and the angle between the cellulose plates was determined with ImageJ [28].

The second occasion was used to image the appearance of tear-out at the breaking point. To see this, we needed to specifically image the glue area. The same camera as in the first setup was used in combination with three close-up lenses (+4, +2, +1 dpt) stacked together (Fig. 5(c)). Video was recorded with same parameters as in the first occasion, but the shutter speed used was 1.5 ms. For the fracture area videos were checked if tear-out is visible between the plates (Fig. 5(b)) and then compared to macro images of the fracture area that were taken after mechanical testing. The capability to slow down the video gives us an opportunity to observe better how the material actually breaks.

3.4. Contact (wetting) angle measurements

An in-house goniometer as depicted in Fig. 6(a) was built to test the camera system suitability for capturing images of droplets for contact angle measurements. The goniometer consists of a high-power LED light source and a 10 mm thick diffusor made of foam, through which the light beam was led towards the sample droplet. A handheld dispenser was used to place a droplet on the substrate which was set on a 0.5 mm graduated ruler of stainless steel attached on a tripod head. Therefore, it was possible to measure the droplet sizes by means of the ruler. Tilt angles were controlled with a digital electronic spirit level with ±0.05° precision. Images/video were then captured with a Raspberry Pi HQ camera module and a CGL 16 mm tele lens. In order to convert the lens to a macro lens, an additional C–CS mount adapter was added as an extension tube. Two stacked C–CS adapters gave 11.6 mm total length of the extension and the minimum focus distance from the lens shortened to 25 mm. The setup was able to illuminate the droplet with uniform and diffuse backlight and resulted in good contrast for the droplet regarding the background as seen in Fig. 6(c) and (d). The images were then analyzed with Opencv2 library to determine the droplet contours that were used for the least square circle fitting. Through this approach, it was possible to compute both the radius and the contact angles at the right and left intersection points of the baseline and the droplet. In addition to these, contact angle measurements were also carried out with the commercial measurement device Biolin Scientific Attension Theta Flex in order to compare and validate the results. For both investigations, Thermo Scientific Finnpipette was used to dispense ∼6 μl ultrapure (type 1) water droplets on PTFE and Fe substrates. It is noteworthy that the water purification was carried out with Synergy UV water purification system. The images in Fig. 6(c) and (d) demonstrate the comparable performance of the present platform based on open-source codes and affordable hardware. This process was followed by measurements of change of droplet height, baseline, volume and contact angles with respect to time. The in-house time lapse script was used to capture the frames in user-defined time intervals. Thereafter, for each captured frame, droplet height and baseline were determined through the pixel-to-millimeters conversion. Since the radius and height were already known, it was possible to compute the droplet volume in terms of spherical cap volume [29].

4. Impact

The modular camera system solution that we have developed can be used for a wide range of applications in the field of experimental mechanics and chemistry. Due to the scripts that are written in Python and open source under MIT licenses as listed in Table 1, it can be used as a platform to integrate Python libraries used for experimental measurements and post-processing. Therefore, the researchers have the freedom to modify the present scripts and insert new ones, which means total control over the system leading to new development concepts in their measurements. In addition, the cost of the setup and the open-source scripts developed for Raspberry Pi and its two different (v2.x and HQ) camera modules make the present system very affordable. As a result of our measurements with valid results, we confidently

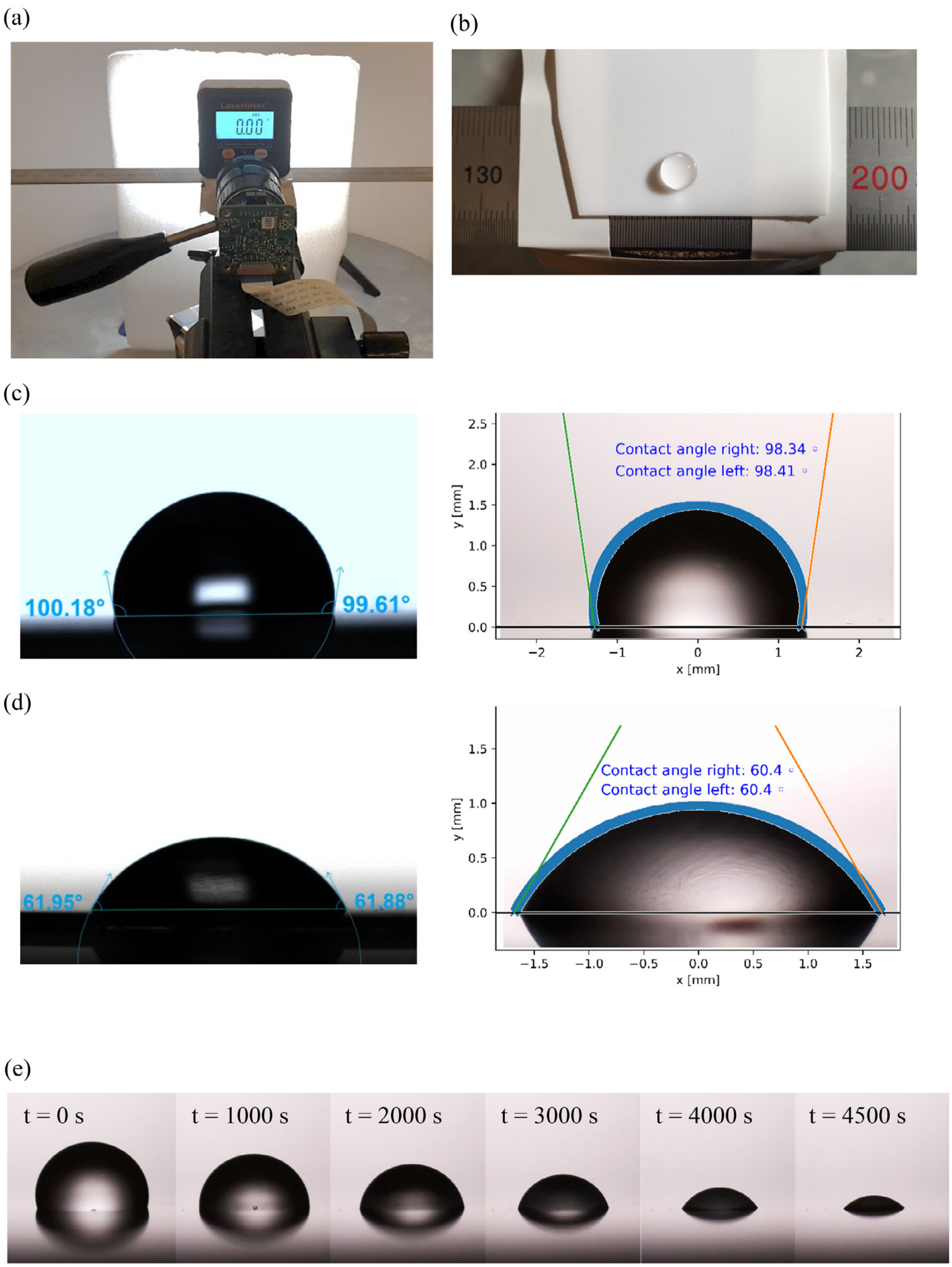

Fig. 6. Contact angle measurement setup and imaging: (a) goniometer with tilt angle calibration by an electronic spirit level, (b) ultra-pure (type 1) water droplet on PTFE plate substrate on a 0.5 mm graduated ruler, (c) comparison of the contact angle measurements ultra-pure (type 1) water droplet on PTFE plate, where the figures on the left show the measurement with commercial device and the figures on the right show the measurement with the introduced setup, modules and scripts, (d) comparison of the contact angle measurements for ultra-pure (type 1) water droplet on Fe plate, where the figures on the left show the measurement with commercial device and the figures on the right show the measurement with the introduced setup, modules and scripts, (e) change of droplet height, baseline, volume and contact angles with respect to time by means of time-lapse photography, (f) change of droplet height, baseline, volume and contact angles with respect to time for a specific time interval.

provided a readily available and easily accessible package for the researchers through GitHub software development platform with the objective of eliminating the inequality of resources in science and engineering worldwide.

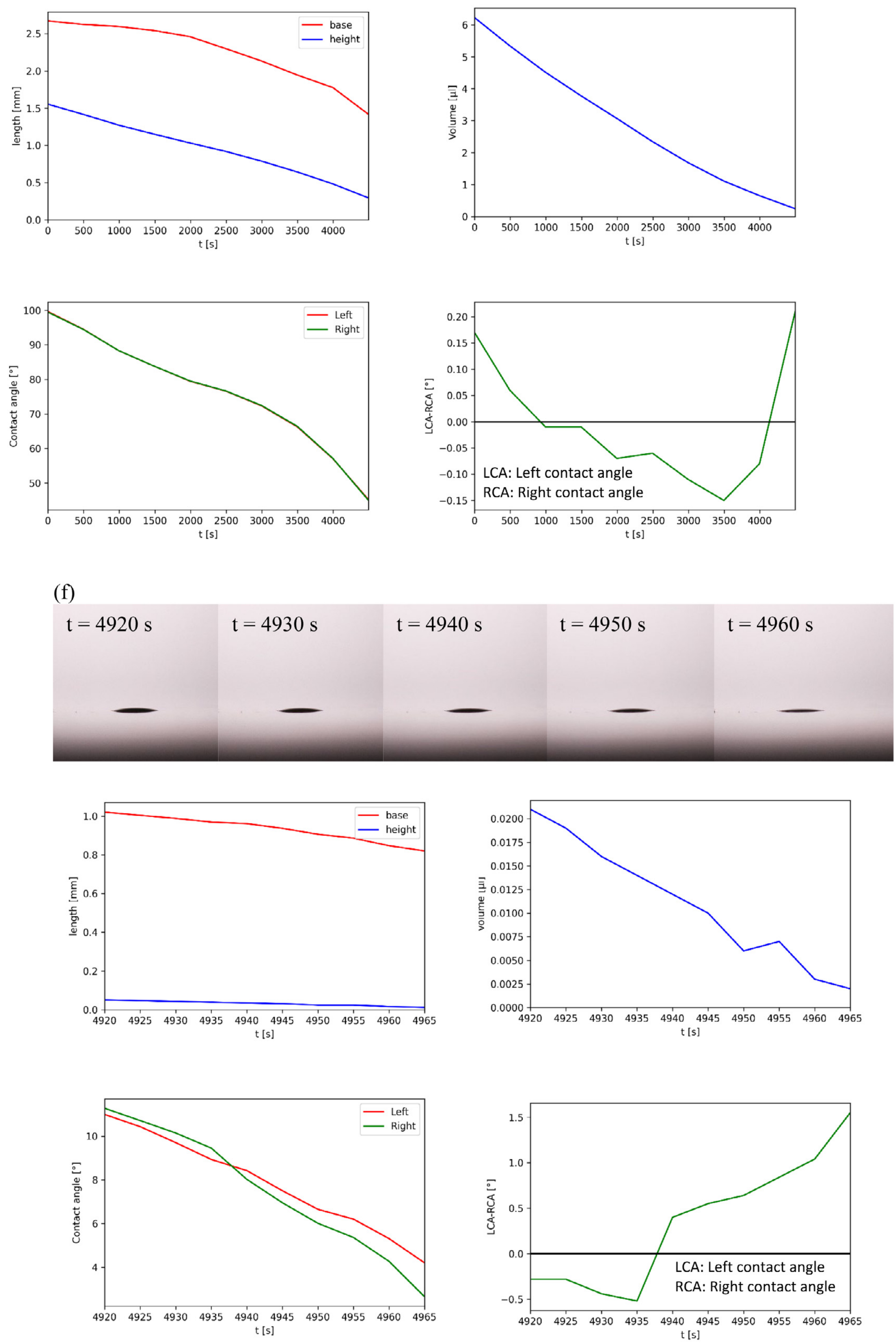

Fig. 6. (*continued*).

5. Conclusions

In this work, we presented a modular and affordable camera setup and software framework using in-house Python scripts that can be integrated with publicly available libraries and packages for experimental measurements. Due to its low cost and high portability, we used Raspberry Pi single board computer as our computing platform. Owing to the recent advancements in the

Raspberry Pi camera modules and compatible optics, we developed several test setups and conducted various experiments in the fields of applied mechanics and chemistry to validate the present system. We expect the provided setups and scripts to be adopted by other researchers, which advances the current state-of-the-art in various fields of science and engineering.

Declaration of competing interest

The authors declare that they have no known competing financial interests or personal relationships that could have appeared to influence the work reported in this paper.

Acknowledgments

KM and AK generated the concept. KM, as the main programmer, and AK wrote the scripts to realize the work. KM, AK and MR conducted DIC owing to Kim Widell at the Department of Mechanical Engineering, Aalto University. DL and JV conducted photoisomerization experiments and the RGB analysis, JT and LL carried out lap shear tests with the high-speed camera option. KM conducted the contact (wetting) angle measurements with Timo Kotilahti and MR. All the authors contributed to the manuscript writing while AK edited and finalized the manuscript. DL and JV gratefully acknowledge the funding from Academy of Finland SUPER-WEAR project (decision number 322214). AK gratefully acknowledges the Research Fellowship at the School of Electrical Engineering and funding from the Academy of Finland BESIMAL project (decision number 334197).

Appendix A. Supplementary materials

The user manual, Python scripts, 3-D printing files for camera mount and adjustment, tutorial materials can be accessed through https://github.com/kmiikki/rpi-camera.

References

[1] Schreier H, Orteu J-J, Sutton MA. Image correlation for shape, motion and deformation measurements. 2009, http://dx.doi.org/10.1007/978-0-387-78747-3.
[2] Karakoç A, Tukiainen P, Freund J, Hughes M. Experiments on the effective compliance in the radial-tangential plane of Norway spruce. Compos Struct 2013;102:287–93.
[3] Mathai PP, Liddle JA, Stavis SM. Optical tracking of nanoscale particles in microscale environments. Appl Phys Rev 2016. http://dx.doi.org/10.1063/1.4941675.
[4] Tofa TS, Kunjali KL, Paul S, Dutta J. Visible light photocatalytic degradation of microplastic residues with zinc oxide nanorods. Environ Chem Lett 2019. http://dx.doi.org/10.1007/s10311-019-00859-z.
[5] Dolan EB, Verbruggen SW, Rolfe RA. Techniques for studying mechanobiology. In: Mechanobiol. Heal. Dis.. 2018, http://dx.doi.org/10.1016/B978-0-12-812952-4.00001-5.
[6] Tekieli M, De Santis S, de Felice G, Kwiecień A, Roscini F. Application of digital image correlation to composite reinforcements testing. Compos Struct 2017. http://dx.doi.org/10.1016/j.compstruct.2016.10.096.
[7] Palanca M, Tozzi G, Cristofolini L. The use of digital image correlation in the biomechanical area: A review. Int Biomech 2016. http://dx.doi.org/10.1080/23335432.2015.1117395.
[8] Pan B, Tian L, Song X. Real-time, non-contact and targetless measurement of vertical deflection of bridges using off-axis digital image correlation. NDT E Int 2016. http://dx.doi.org/10.1016/j.ndteint.2015.12.006.
[9] Andre D. PyDic, (N.D.). Universite de Limoges; 2020, (accessed September 8, 2020) www.unilim.fr=pages_perso=damien.andre=index.html.
[10] Belloni V, Ravanelli R, Nascetti A, Di Rita M, Mattei D, Crespi M. Py2dic: A new free and open source software for displacement and strain measurements in the field of experimental mechanics. Sensors (Switzerland) 2019. http://dx.doi.org/10.3390/s19183832.
[11] Olufsen SN, Andersen ME, Fagerholt E. μDIC: An open-source toolkit for digital image correlation. SoftwareX 2020. http://dx.doi.org/10.1016/j.softx.2019.100391.
[12] Turner DZ. An Overview of the Gradient-Based Local DIC Formulation for Motion Estimation in DICe. Sandia Report, SAND2016-7360 R.; 2016.
[13] Blaber J, Adair B, Antoniou A. Ncorr: Open-source 2D digital image correlation matlab software. Exp Mech 2015. http://dx.doi.org/10.1007/s11340-015-0009-1.
[14] Dong YL, Pan B. A review of speckle pattern fabrication and assessment for digital image correlation. Exp Mech 2017. http://dx.doi.org/10.1007/s11340-017-0283-1.
[15] Belloni V, Ravanelli R, Nascetti A, Di Rita M, Mattei D, Crespi M. Digital image correlation from commercial to FOS software: A mature technique for full-field displacement measurements. In: Int. Arch. Photogramm. Remote Sens. Spat. Inf. Sci. - ISPRS Arch. 2018, http://dx.doi.org/10.5194/isprs-archives-XLII-2-91-2018.
[16] Özkan M, Borghei M, Karakoç A, Rojas OJOJ, Paltakari J. Films based on crosslinked TEMPO-oxidized cellulose and predictive analysis via machine learning. Sci Rep 2018;8. http://dx.doi.org/10.1038/s41598-018-23114-x.
[17] Hebbar RS, Isloor AM, Ismail AF. Contact angle measurements. In: Membr. Charact.. 2017, http://dx.doi.org/10.1016/B978-0-444-63776-5.00012-7.
[18] Law KY, Zhao H. Surface wetting: Characterization, contact angle, and fundamentals. 2015, http://dx.doi.org/10.1007/978-3-319-25214-8.
[19] Huhtamäki T, Tian X, Korhonen JT, Ras RHA. Surface-wetting characterization using contact-angle measurements. Nat Protoc 2018. http://dx.doi.org/10.1038/s41596-018-0003-z.
[20] Favier B, Chamakos NT, Papathanasiou AG. A precise goniometer/tensiometer using a low cost single-board computer. Meas Sci Technol 2017. http://dx.doi.org/10.1088/1361-6501/aa8e25.
[21] Nežerka V, Somr M, Trejbal J. Contact angle measurement tool based on image analysis. Exp Tech 2018. http://dx.doi.org/10.1007/s40799-017-0231-0.
[22] van Gorcum M. Dynamics of Soft Wetting. University of Twente; 2019, http://dx.doi.org/10.3990/1.9789036547376.
[23] Launay G. Pydsa: Drop shape analysis in python. 2018, https://Framagit.Org/Gabylaunay/PyDSA_gui.
[24] International Organization for Standardization, ISO 527-1:2012 - Plastics – Determination of tensile properties – Part 1: General principles, Geneva, 2012.
[25] Ahrens J, Geveci B, Law C. Paraview: An end-user tool for large-data visualization. In: Vis. Handb.. 2005, http://dx.doi.org/10.1016/B978-012387582-2/50038-1.
[26] Kohl-Landgraf J, Braun M, Özçoban C, Gonçalves DPN, Heckel A, Wachtveitl J. Ultrafast dynamics of a spiropyran in water. J Am Chem Soc 2012. http://dx.doi.org/10.1021/ja304395k.
[27] Abbott S. Adhesion Science: Principles and Practice. Lancaster, Pennyslvania: DEStech Publications; 2015.
[28] Schneider CA, Rasband WS, Eliceiri KW. NIH image to imageJ: 25 years of image analysis. Nat Methods 2012. http://dx.doi.org/10.1038/nmeth.2089.
[29] Handbook of Mathematics and Computational Science, Choice Rev. Online. 1999, http://dx.doi.org/10.5860/choice.36-2801.